Quasiclassical Trajectory Calculations of the N(2D) + H2O Reaction Elucidating the Formation Mechanism of HNO and HON Seen in Molecular Beam Experiments

ARTICLE *in* JOURNAL OF PHYSICAL CHEMISTRY LETTERS · OCTOBER 2014

Impact Factor: 7.46 · DOI: 10.1021/jz501757s

4 AUTHORS:

Zahra Homayoon
Emory University
18 PUBLICATIONS **98** CITATIONS
SEE PROFILE

Joel M Bowman
Emory University
542 PUBLICATIONS **15,195** CITATIONS
SEE PROFILE

Nadia Balucani
Università degli Studi di Perugia
163 PUBLICATIONS **3,481** CITATIONS
SEE PROFILE

Piergiorgio Casavecchia
Università degli Studi di Perugia
168 PUBLICATIONS **4,332** CITATIONS
SEE PROFILE

THE JOURNAL OF PHYSICAL CHEMISTRY Letters

Letter

pubs.acs.org/JPCL

Quasiclassical Trajectory Calculations of the N(^{2}D) + H_2O Reaction Elucidating the Formation Mechanism of HNO and HON Seen in Molecular Beam Experiments

Zahra Homayoon,*[,†] Joel M. Bowman,*[,†] Nadia Balucani,*[,‡] and Piergiorgio Casavecchia*[,‡]

[†]Department of Chemistry and Cherry L. Emerson Center for Scientific Computation, Emory University, Atlanta, Georgia 30322, United States

[‡]Dipartimento di Chimica, Biologia e Biotecnologie, Università degli Studi di Perugia, 06123 Perugia, Italy

Supporting Information

ABSTRACT: The N(^{2}D) + H_2O is a reaction with competitive product channels, passing through several intermediates. Dynamics of this reaction had been investigated by two of the present authors at two collision energies, E_c, using the crossed molecular beams mass spectrometric method (*Faraday Discuss.* **2001**, *119*, 27−49). The complicated mechanism of this reaction and puzzling results encouraged us to investigate the reaction in a joint experimental/theoretical study. Quasiclassical trajectory (QCT) calculations on an ab initio potential energy surface describing all channels of the title reaction are done with a focus on the N/H exchange channels. Interesting results of QCT calculations, in very good agreement with experimental data, reveal subtle details of the reaction dynamics of the title reaction to HNO/HON + H exit channels by disentangling the different routes to formation of the two possible HNO/HON isomers and therefore assisting in a critical manner the derivation of the reaction mechanism. Results of the present study show that the nonstatistical HNOH intermediate governs exit channels; therefore, the HON channel is as important as that of HNO. The study also confirms that the H_2 + NO molecular channel is negligible even though the barrier to its formation is calculated to be well below the reactant asymptote.

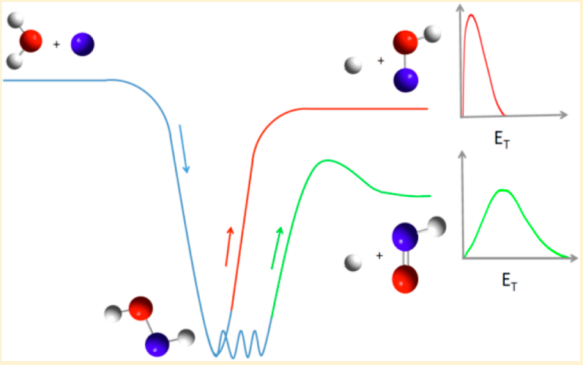

SECTION: Kinetics and Dynamics

Theoretical/computational chemistry has emerged as an important tool to help elucidate chemical processes. Quasiclassical trajectory (QCT) and quantum mechanical (QM) scattering methods using accurate potential energy surfaces (PESs) for noncompeting product channels in simple (i.e., three-atom, four-atom, and six-atom) direct reactions have deeply advanced our understanding of chemical reactivity[1−3] in its basic aspects. Nevertheless, experimental and theoretical investigations of the dynamics of more complex polyatomic reactions, with numerous competing product channels, still represent a major challenge for both experiment and theory. Recent combined experimental/theoretical studies by us of the polyatomic multichannel nonadiabatic reaction of ground-state oxygen atoms, O(^{3}P), with ethylene, C_2H_4, have proved that theory (QCT surface-hopping calculations on full-dimensional ab initio coupled triplet/singlet PESs) has reached the capability to reproduce well the experimental findings (primary products and branching ratios) including detailed observables, such as product angular and translational energy distributions obtained in crossed molecular beam (CMB) reactive scattering experiments;[4] this study arguably represents the current benchmark in this research area. However, even for the H + H_2 reaction, recent joint experimental/theoretical studies have revealed surprising and unexpected dynamical pathways.[5,6] Another class of complicated cases is competition of several channels of isomers effectively bypassing deep intermediates. Theoretically, construction of the underlying complicated PESs is challenging due to the huge amount of electronic structure calculations needed to describe channels of interest while the scattering calculations are made complex by the large number of degrees of freedom. Experimentally, the CMB method with mass spectrometric (MS) detection is best suitable because of universal detection, but the identification of isomeric products (with the same mass-to-charge ratio, m/z) is only possible in favorable cases, when the formation mechanism and formation enthalpies are significantly different. Because in many reactions of practical importance it is crucial to derive the product branching ratio where also isomers are distinguished, CMB-MS experiments on indirect polyatomic multichannel reactions are often complemented by electronic structure calculations of the PES stationary points (transition states and minima, i.e., bound intermediates) and statistical estimates of the product

Received: August 20, 2014
Accepted: September 29, 2014

   dx.doi.org/10.1021/jz501757s | *J. Phys. Chem. Lett.* 2014, 5, 3508−3513

branching ratio. Statistical methods are applicable when one or more strongly bound intermediates are formed after the initial interaction of the reactants (e.g., addition or insertion) and rely on several approximations, among which the most important one is that the energy is quickly randomized along all of the degrees of freedom of the intermediate(s). Statistical methods do not really describe the reaction dynamics, that is, they do not follow the reaction in its becoming, but only the evolution of highly excited reaction intermediates. Yet, valuable information is obtained, and assistance in the interpretation of the scattering results is furnished. Nevertheless, in many reactive systems, important dynamical effects have been noted, and statistical methods fail.[7−9] In particular, when more than one intermediate can be directly formed by the reactants' interaction (for instance, addition of a radical on different sites of a molecule or insertion into more than one bond), only a dynamical treatment of the entrance channels can really describe the reactive system and lead to the correct determination of the product branching ratio.[10−12]

In this Letter, we apply a rigorous QCT approach to the study of a prototype reaction that exhibits the above challenging characteristics, namely, the reaction of excited nitrogen atoms, $N(^2D)$, with the water molecule. Five products channels

$$N(^2D) + H_2O \rightarrow HNO + H \quad \Delta H^0_0 = -40.9 \text{ kcal mol}^{-1} \quad (1)$$

$$\rightarrow HON + H \quad \Delta H^0_0 = -7.2 \text{ kcal mol}^{-1} \quad (2)$$

$$\rightarrow OH + NH \quad \Delta H^0_0 = -17.4 \text{ kcal mol}^{-1} \quad (3)$$

$$\rightarrow NO + H_2 \quad \Delta H^0_0 = -95.2 \text{ kcal mol}^{-1} \quad (4)$$

$$\rightarrow O + NH_2 \quad \Delta H^0_0 = -11.7 \text{ kcal mol}^{-1} \quad (5)$$

are accessible at low collision energies of the reactants by passing through deep intermediates, as shown in Figure 1. At first glance, this system represents an ideal case for the application of statistical approaches. The present QCT calculations thus provide a test of the validity of statistical approaches against a dynamical treatment. It is to be noted that this reaction is responsible for the nitrogen−oxygen chemistry coupling on the upper atmosphere of Titan[13] and can also take

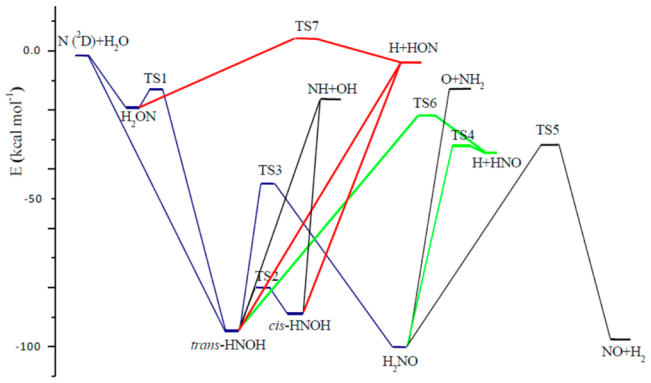

Figure 1. Energy schematic for the fitted PES of the $N(^2D) + H_2O$ reaction pathways used in the present study. A complete schematic with detailed relative energies is given in the Supporting Information (SI) (Figure S1). Blue lines show the entrance channel of reactants making H_2ON and then *trans*- and *cis*-HNOH and H_2NO intermediates. Intermediates could dissociate into five exit channels. More details of the PES are given in the SI.

place in the terrestrial atmosphere during thunderstorms, therefore contributing to the natural NO budget.[14]

The stationary points of the global H_2NO PES have already been investigated in previous studies.[15−19] Very recently, two of the authors developed a global PES for the $N(^2D) + H_2O$ reaction, with a data set of 312 000 electronic energies at a high level of theory.[20] The PES accurately describes stationary points and minimum-energy pathways. The new PES has been tested with QCT calculations of channel 3 leading to OH + NH products. The internal energy distributions of products were found to be in a good agreement with experimental data.[21] As shown in Figure 1, the reaction proceeds though the formation of a bound intermediate, *trans*-HNOH, which can isomerize to other intermediates (*cis*-HNOH or H_2NO) or decompose into products. As for the N/H exchange channels, dissociation of *trans*-HNOH and H_2NO intermediates via TS6 and TS4, respectively, can generate HNO + H, while the production of the HON isomer takes place through dissociation of *cis*- and *trans*-HNOH intermediates with no barrier and also via dissociation of H_2ON by passing through TS7.

In 2001, two of the present authors investigated the dynamics of the $N(^2D) + H_2O$ reaction at two collision energies, E_c, using the CMB-MS method and provided a preliminary report[22] on the H-displacement channel at the higher E_c of about 12 kcal/mol. The experimental data were interpreted as follows: (i) the occurrence of the H_2 molecular elimination channel 4 leading to NO + H_2 was ruled out; (ii) most of the recorded reactive scattering signal was attributed to channel 1, whose reaction enthalpy is in line with the high-energy tail of the best-fit product translational energy distribution, $P(E_T)$; (iii) a direct abstraction mechanism leading to the formation of the HON isomer following N attack on the O atom of water was invoked to account for some backward-scattered product density at the higher E_c investigated. To inquire further about the possible occurrence of the NO + H_2 channel, we have performed more scattering experiments, but the results turned out to be very puzzling (see below) and challenged our previous interpretation[22] of the dynamics of the $N(^2D) + H_2O$ reaction.

Here, we report on QCT calculations of the product translational energy and angular distributions for the two different channels leading to HNO/HON products and new CMB experimental data. The QCT results are converted into the laboratory (LAB) system of coordinates and averaged over the experimental conditions for a direct comparison with the CMB distributions. Important insights have been obtained that reveal the detailed mechanism of the $N(^2D) + H_2O$ reaction.

A description of the experimental setup is given in the Supporting Information (SI). In the first series of experiments,[22] reactive signal was observed at $m/z = 30$, with a very small signal being noted also at $m/z = 31$. However, the signal-to-noise ratio (S/N) at $m/z = 31$ was too low to permit measurements of product angular and velocity distributions. The $m/z = 31$ signal is associated with parent ions HNO^+ and/or HON^+ from the HNO/HON + H channels 1 and 2, while that at $m/z = 30$ can originate from both the NO^+ parent ion of the NO + H_2 channel 4 and the daughter ion NO^+ from the HNO/HON + H channels. Data analysis led us to the conclusion that the $m/z = 30$ distributions were actually associated exclusively with the NO^+ daughter ion from HNO/HON. The reason why the signal at $m/z = 30$ cannot be attributed to the NO + H_2 channel is that the H_2 elimination channel is strongly exoergic and characterized by a very high

dx.doi.org/10.1021/jz501757s | J. Phys. Chem. Lett. 2014, 5, 3508−3513

exit barrier. Because of linear momentum conservation, its angular distribution should be significantly wider than the one effectively recorded in CMB experiments. (In CMB-MS experiments, the measurements of angular and velocity distributions can be assigned to a given product even when its parent ion is not observable because of energy and momentum conservation (Lee, Y. T. *Molecular Beams Methods*; 1987).) Because the experimental product translational energy distribution, $P(E_T)$, extends to ~45 kcal/mol (see Figure 9 in ref 22), by considering the reaction enthalpies of channels 1 and 2, the signal recorded at m/z = 30 was attributed to HNO formation. This is a common procedure in CMB experiments, according to which the reactive signal is attributed to the channel with the reaction enthalpy in line with the high-energy tail of $P(E_T)$.[6−8,10] Nonetheless, some uncertainty remained on our conclusions because of the missing data for the parent ion HNO^+/HON^+ distributions.

When we finally succeeded in measuring the product angular and velocity distribution also at the parent mass of HNO/HON (m/z = 31), to our surprise, the m/z = 31 angular distribution at E_c = 12.2 kcal/mol was found to be significantly wider than that measured at m/z = 30. Angular distributions at the two masses for E_c = 12.2 kcal/mol are shown comparatively in Figure 2, while the corresponding TOF data at selected LAB

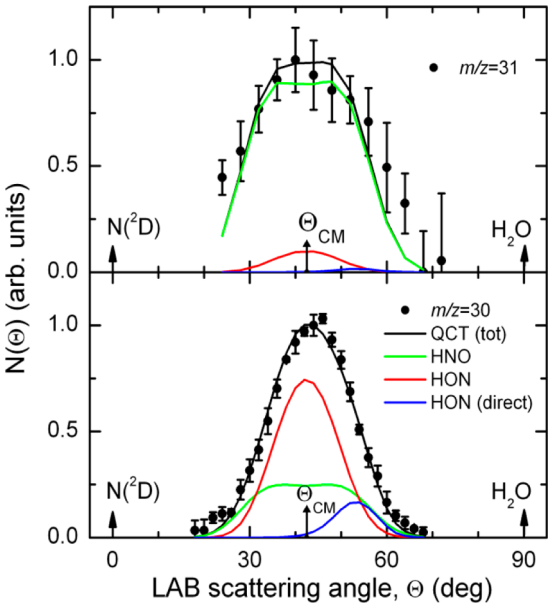

Figure 2. LAB angular distribution at m/z = 31 (top panel) and 30 (bottom panel) for the N(^{2}D) + H_2O reaction at E_c = 12.2 kcal/mol. Symbols as indicated: ● experimental point with standard deviation; black line: global best-fit; green line: HNO from the HNOH long-lived intermediate; red line: HON from the HNOH long-lived intermediate; blue line: HON from the direct process. All of the lines represent simulations performed using the QCT results (see the text).

angles are depicted in Figures 3 (m/z = 31) and 4 (m/z = 30). The angular distribution for E_c = 7.5 kcal/mol at m/z = 30 is shown in Figure 5, and the corresponding TOF spectra are given in Figure S8 (SI). All of the lines in Figures 2−5 are the result of theoretical simulations using the QCT results (see below). The reactive scattering signal at m/z = 31 is less than 10% of that at m/z = 30 at E_c = 12.2 kcal/mol, while at E_c = 7.5 kcal/mol, it was so low that the m/z = 31 distributions could not be measured (this is due to the much lower H_2O beam

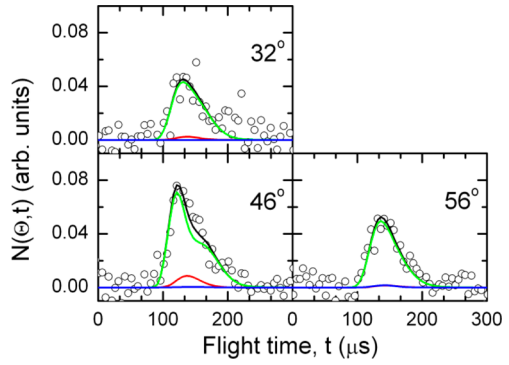

Figure 3. m/z = 31 product TOF distributions at the indicated LAB angles for the N(^{2}D) + H_2O reaction at E_c = 12.2 kcal/mol. Symbols are as those in Figure 2.

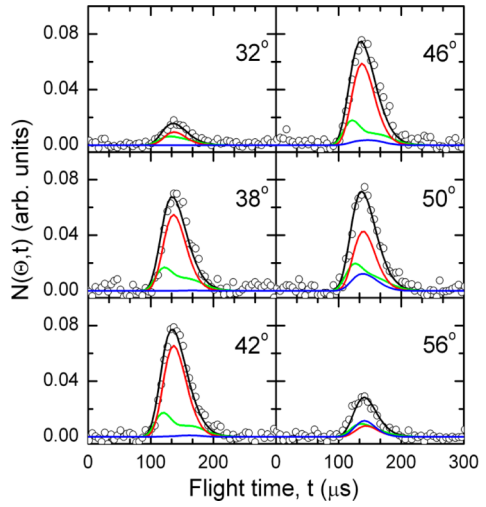

Figure 4. m/z = 30 product TOF distributions at the indicated LAB angles for the N(^{2}D) + H_2O reaction at E_c = 12.2 kcal/mol. Symbols are as those in Figures 2 and 3.

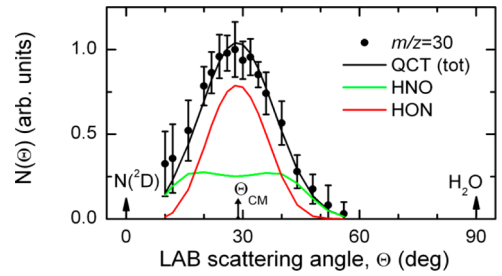

Figure 5. LAB angular distribution at m/z = 30 and E_c = 7.5 kcal/mol. Symbols are as those in Figure 2.

intensity under the experimental conditions of the experiment at 7.5 kcal/mol; see the SI). If all of the products attributed to this mass were coming from dissociative ionization of HNO/HON primary products, as suggested in our previous work,[22] the m/z = 30 and 31 distributions would have been identical because the daughter ion distributions must be identical to those of the parent ion. In addition, if the reason for the difference were associated with the contribution of channel 4 to the m/z = 30 distributions, even in the case that only a relatively small fraction of H_2 channel was formed, the m/z = 30 distribution would have been wider. This is the opposite of the experimental observation that clearly shows that the m/z =

dx.doi.org/10.1021/jz501757s | J. Phys. Chem. Lett. 2014, 5, 3508−3513

30 angular distribution (Figure 2, bottom panel) is actually significantly narrower than that at m/z = 31 (Figure 2, top panel).

These results are puzzling. The fact that the dominant parts of the angular distributions at the two masses, centered around the center-of-mass (CM) angle, are of different width, as described above, can only be explained if at least two dynamically different channels contribute to the m/z = 31 signal and if the corresponding products fragment to m/z = 30 in a very different way. These two dynamically different channels are the considerably exoergic HNO + H channel coming from the decomposition of the HNOH intermediate via cleavage of the O−H bond and the weakly exoergic HON + H channel coming also from decomposition of the HNOH intermediate but via N−H bond cleavage. Also, H_2NO can give decomposition to HNO + H. We could not discriminate the two isomers during the best-fit procedure by relying only on the experimental data. This is due to the fact that, as we are going to see, the CM angular distributions are the same.

The goal of quasiclassical calculations is to do reliable calculations initiated from reactants and investigate channels leading to N/H exchange. This is possible by performing calculations on an accurate PES. The PES is fit to a large data set of electronic energies, most at the UCCSD(T)-F12/aug-cc-pVTZ level of theory using a basis of permutationally invariant polynomials in Morse-like variables in all of the internuclear distances, as described in detail elsewhere.[23] Details of the PES are given in the SI. Figure 1 presents the schematic of the multichannel PES for the $N(^2D)$ + H_2O reaction. Entrance channel and formation pathways of four intermediates are shown with blue lines. We also highlight the dissociation pathways of intermediates to HNO + H and HON + H products. A more detailed figure with the all-stationary points included is given in Figure S1 (SI). Also, a detailed description of the PES is given in the SI. The QCT calculations were performed at the two different collision energies of 7.5 and 12.2 kcal/mol corresponding to the present experiments; 400 000 trajectories were run per energy. The trajectories were propagated with the time step of 0.12 fs for a maximum of 500 000 time steps. More details about QCT calculations are available in the SI.

As seen in Figure 1, the H/N exchange channels leading to HNO and HON pass through the same intermediates, *cis*- and *trans*-HNOH. Specifically, the goal of QCT calculations is to obtain translational energy and angular distributions of HNO + H and HON + H channels and also the branching ratio of products.

The CM angular distributions from the QCT calculations for the two main channels, namely, HNO + H and HON + H, were found to be isotropic, that is, backward−forward symmetric with constant intensity over the entire 0−180° angular range. However, the theoretical translational energy distributions for these two channels were found to be dramatically different, as can be seen from the Figures 6 and S5 (SI). Specifically, the $P(E_T)$ for HNO + H was found to peak, at the highest E_c, at about 18 kcal/mol and to extend to the limit (about 44 kcal/mol) of energy conservation. In contrast, the $P(E_T)$ for the HON + H channel was found to rise from zero very quickly and peak at about 4 kcal/mol and extend within the limit (about 20 kcal/mol) of energy conservation for this channel. Similar behavior is found from the QCT results also at the lower E_c of 7.5 kcal/mol (see Figure S5 in the SI). The branching ratio of cross sections $\sigma(HNO)/[\sigma(HNO) + \sigma(HON)]$ is found to be about 0.59 at low E_c and 0.48 at the high E_c (see the SI). With these QCT results transformed into the LAB system and averaged over experimental conditions (see the SI), we obtained an excellent simulation of both the angular and TOF distributions at low E_c, as can be seen from Figures 5 and S8 (SI). For the higher E_c, the calculated LAB angular distribution was somewhat less backward-distributed than the experiment (see Figure S6, SI), and in order to reproduce the slight backward bias of the experimental distribution, it was necessary to also account for another source of the HON + H channel (see Figures 2 and S6, SI) that arises from direct decomposition, via TS7, of the H_2ON initial intermediate formed from the direct attack of the N atom on the O side of the water molecule (see Figure 1). As can be seen in Figure S7 (SI), this pathway is characterized by a $P(E_T)$ distribution that is very different from that of the HON + H channel arising from the barrierless decomposition of the *trans*/*cis*-HNOH intermediate. The HON translational energy distribution shown in Figure S7 (SI) was obtained by running trajectories initiated at TS7. As seen, it peaks at around 18 kcal/mol and then falls off abruptly, which is typical of a direct process, in contrast to the translational energy distribution shown in Figure 6, which peaks at 4 kcal/mol but which has a tail slightly beyond 20 kcal/mol. Note, at the lower collision energy of 7.5 kcal/mol, the HON $P(E_T)$ distribution is zero at around 18 kcal/mol. Therefore , we speculate that at the 12.2 kcal/mol collision energy, there is a minor contribution from the pathway via TS7 to the HON product. For this pathway, the angular distribution was not obtained from QCT but was derived from a best-fit procedure where the only variable

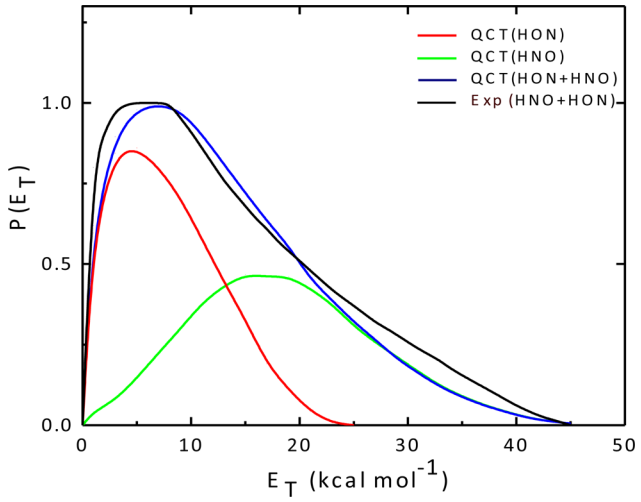

Figure 6. Translational energy distribution of HNO + H, HON + H, and the sum of these channels from QCT compared with experimental results (continuous black line) at E_c = 12.2 kcal/mol. The continuous line is very similar to that derived in our earlier fit of the m/z = 30 data assuming only one pathway leading to HNO + H products (ref 22). As can be seen, the QCT analysis has permitted to us disentangle that actually the previously derived $P(E_T)$ is an envelope of two very different contributions, one corresponding to the HNO product and the other to the HON product, both formed via a long-lived complex mechanism starting from the same long-lived HNOH complex that can decompose via two dynamically very different pathways, a barrierless one involving N−H bond cleavage and the other occurring via TS6 and involving O−H bond cleavage. HNO could also be produced through an isomerization channel to H_2NO and subsequent dissociation.

dx.doi.org/10.1021/jz501757s | J. Phys. Chem. Lett. 2014, 5, 3508−3513

quantities were the $T(\theta)$ shape and the relative weight of this contribution. A CM angular distribution backward-peaked (see Figure S7, SI), and a ratio ($HON_{direct}/HON_{indirect}$) of 0.15 allowed us to reach an accurate simulation of the experimental results (see Figure 2, bottom panel, and Figure 4). The CM functions of the backward-peaked contribution depicted in Figure S7 (SI) are very similar to those invoked by us in the earlier work[22] to rationalize the appearance of a backward-scattering bias at high E_c. Finally, note that the HON + H pathway is directly accessible from shallow H_2ON, and therefore, the dynamics via this pathway would resemble the "trapped abstraction" pathway recently reported for the $O(^1D)$ + CH_4 reaction.[24]

It is interesting to note that from the QCT simulations of the m/z = 31 data (see Figure 2, top panel), it is seen that most of the signal is coming from the HNO isomer contribution, while little is from the HON isomer. This indicates that the HON isomer fragments to NO^+ (m/z = 30) much more than the HNO isomer, that is, the HNO^+ ion is much more stable than the HON^+ ion. In this regard, it is worth noting that from early MS studies of the kinetics of the H + NO reaction, it was concluded that HNO contributes greatly to m/z = 30 upon electron impact at 70 eV (a value very close to ours of 60 eV), with a fragmentation ratio (m/z = 31)/(m/z = 30) of about 0.03.[25] Furthermore, energy-dependent photoionization mass spectra studies of hydroxylamine (NH_2OH)[26] confirmed previous high-level theoretical work[27] that the HNO^+ isomer is more stable by about 13 kcal/mol with respect to HON^+. This leads us to expect that HON fragments more extensively than the HNO isomer upon ionization. Our observations are fully consistent with these relative stabilities of HNO^+ and HON^+ ions; in fact, the fraction of HON^+ that survives at m/z = 31 is much smaller than the fraction of HNO^+ (see Figure 2).

Theoretically, channels leading to H_2 + NO products (related to m/z = 30) were also considered. Overall, they were found to be very minor channels. Conventionally, TS5 connects H_2NO to the H_2 + NO products, in which the PES involves that pathway. Nevertheless, the possibility of roaming H-atom pathways to abstract a H atom from incipient HNO and HON fragments from dissociation of H_2NO and HNOH intermediates was considered. Such pathways were found, and they are shown in the SI (Figure S2). Although the PES describes those pathways, as noted, they operate in a very minor way that seems reasonable at the available energy of fragments.

We also consider other aspects of HNO/HON product channels. Figure S3 (SI) shows the comparison of the lifetimes of trajectories that lead to HNO and HON at two different energies. The average lifetime for HNO is 1.03 ps compared with 0.59 ps for HON at 12.2 kcal/mol. We also present the potential energy along two sample trajectories leading to HNO and HON in Figure S4 (SI). As seen, the time history of these trajectories is quite different. The trajectory leading to HNO clearly shows complex formation, whereas the one leading to HON is much more direct, with just transient complex formation. This suggests that the reaction mechanism is perhaps more statistical for the HNO product than that for the HON one. This would imply that a statistical treatment of the branching ratio of these product channels might be in error. To investigate this, we performed 40 000 trajectories initiated at HNOH using random microcanonical sampling at three different energies, consistent with 12.2, 7.5, and 1.5 kcal/mol E_c's. The 1.5 kcal/mol is compared with an unpublished branching ratio of HNO/HON products of ref 20. These were predominantly long-lived and hence "statistical" trajectories. Comparison of the branching ratio of HON at different energies from two different sets of trajectories is presented in Table 1. At 1.5 kcal/mol for the $N(^2D)$ + H_2O reaction, the

Table 1. Branching Ratio, $\sigma(HON)/[\sigma(HNO) + \sigma(HON)]$, of HON Products from Trajectories Initiated from Reactants or the *trans*-HNOH Intermediate at Three Different Energies

	E = 1.5 kcal/mol	E = 7.5 kcal/mol	E = 12.2 kcal/mol
N + H_2O	0.40	0.41	0.52
trans-HNOH	0.15	0.21	0.23

branching ratio of HON is 0.4, compared with 0.15 from dissociation of HNOH. As seen at 7.5 and 12.2 kcal/mol collision energies, contribution of HON from the title reaction is about two times bigger than direct dissociation of HNOH. Thus, the bimolecular trajectories lead to significantly more HON than is found from unimolecular/statistical ones initiated at the HNOH minimum. Generalizing the present results, we can conclude that the presence of a deep well associated with a strongly bound intermediate is a necessary but not a sufficient condition to achieve energy randomization. This can affect not only the product energy release, as previously observed[28] for simple reactions like $O(^1D)$ + H_2, but also a more global feature such as the product branching ratio of multichannel reactions. The reactive system investigated here, however, involves four light atoms, and the deviations between statistical and dynamical treatments may be smaller in more complex systems. It would certainly be interesting to investigate this point in the future.

Another aspect of this work deserves attention. In the interpretation of the CMB results of ref 22, the m/z = 30 signal was attributed almost completely to channel 1. The comparison between the experimental and QCT results clearly puts a warning that the common procedure in CMB experiments to attribute the reactive signal to the channel with the variation of enthalpy in line with the maximum value assumed by product E_T can lead to serious mistakes. Important contributions coming from less exothermic channels leading to isomeric products can be embedded in the global product translational energy distribution.

In conclusion, excellent agreement between theoretical and experimental results of total translational energy and angular distributions of the $N(^2D)$ + H_2O → H + HNO/HON reaction is seen. HNO and HON channels show very different distribution of translational energy, where none of them separately but the sum of them with the branching ratio of QCT results could reproduce experimental results. In contrast with the first interpretation of experimental results, the HON + H channel has a significant contribution. Statistical behavior of the deep intermediate, HNOH, has been investigated by running trajectories initiated at the HNOH with the random distribution of available energy. Significant differences between the branching ratio of products started from the reactants or intermediate propose that a dynamical treatment is necessary to describe this reactive system.

In addition, this work suggests that the attribution of the CMB reactive signal only on the basis of the maximum value assumed by the product $P(E_T)$ can lead to erroneous

dx.doi.org/10.1021/jz501757s | J. Phys. Chem. Lett. 2014, 5, 3508−3513

conclusions by neglecting important contributions coming from less exothermic channels leading to isomeric products.

■ ASSOCIATED CONTENT

Supporting Information

Details of the experiment, the potential energy surface, and quasiclassical trajectory calculations. This material is available free of charge via the Internet at http://pubs.acs.org.

■ AUTHOR INFORMATION

Corresponding Authors

*E-mail: zhomayo@emory.edu (Z.H.).
*E-mail: jmbowma@emory.edu (J.M.B.).
*E-mail: nadia.balucani@unipg.it (N.B.).
*E-mail: piergiorgio.casavecchia@unipg.it (P.C.).

Notes

The authors declare no competing financial interest.

■ ACKNOWLEDGMENTS

J.M.B. and Z.H. thank the Army Research Office (W911NF-11-1-0477) for financial support. N.B. and P.C. thank the Italian MIUR (PRIN 2010-2011, Grant 2010ERFKXL) for financial support.

■ REFERENCES

(1) Wang, X.; Dong, W.; Xiao, C.; Che, L.; Ren, Z.; Dai, D.; Wang, X.; Casavecchia, P.; Yang, X.; Jiang, B.; et al. The Extent of Non-Born−Oppenheimer Coupling in the Reaction of Cl(^{2}P) with para-H_2. *Science* **2008**, *322*, 573−576.

(2) Xiao, C.; Xu, X.; Liu, S.; Wang, T.; Dong, W.; Yang, T.; Sun, Z.; Dai, D.; Xu, X.; Zhang, D. H.; et al. Experimental and Theoretical Differential Cross Sections for a Four-Atom Reaction: HD + OH → H_2O + D. *Science* **2001**, *333*, 440−442.

(3) Czakó, G.; Bowman, J. M. Dynamics of the Reaction of Methane with Chlorine Atom on an Accurate Potential Energy Surface. *Science* **2001**, *334*, 343−346.

(4) Fu, B.; Han, Y.; Bowman, J. M.; Angelucci, L.; Balucani, N.; Leonori, F.; Casavecchia, P. Intersystem Crossing and Dynamics in O(^{3}P) + C_2H_4 Multichannel Reaction: Experiment Validates Theory. *Proc. Natl. Acad. Sci. U.S.A.* **2012**, *109*, 9733−9738.

(5) Jankunas, J.; Zare, R. N.; Bouakline, F.; Althorpe, S. C.; Herráez-Aguilar, D.; Aoiz, F. J. Seemingly Anomalous Angular Distributions in H + D_2 Reactive Scattering. *Science* **2012**, *336*, 1687−1690.

(6) Jankunasa, J.; Snehaa, M.; Zare, R. N.; Bouaklineb, F.; Althorpec, S. C.; Herráez-Aguilard, D.; Aoiz, F. J. Is the Simplest Chemical Reaction Really So Simple? *Proc. Natl. Acad. Sci. U.S.A.* **2014**, *111*, 15−20.

(7) Leonori, F.; Skouteris, D.; Petrucci, R.; Casavecchia, P.; Rosi, M.; Balucani, N. Combined Crossed Beam and Theoretical Studies of the C(^{1}D)+CH_4 Reaction. *J. Chem. Phys.* **2013**, *138*, 024311/1.

(8) Balucani, N.; Bergeat, A.; Cartechini, L.; Volpi, G. G.; Casavecchia, P.; Skouteris, D.; Rosi, M. Combined Crossed Molecular Beam and Theoretical Studies of the N(^{2}D)+CH_4 Reaction and Implications for Atmospheric Models of Titan. *J. Phys. Chem. A* **2009**, *113*, 11138−11152.

(9) Sun, L.; Song, K.; Hase, W. L. A S_N2 Reaction that Avoids Its Deep Potential Energy Minimum. *Science* **2002**, *296*, 875−878.

(10) Leonori, F.; Petrucci, R.; Wang, X.; Casavecchia, P.; Balucani, N. A Crossed Beam Study of the Reaction CN+C_2H_4 at a High Collision Energy: The Opening of a New Reaction Channel. *Chem. Phys. Lett.* **2012**, *553*, 1−5.

(11) Maity, S.; Parker, D. S. N.; Kaiser, R. I.; Ganoe, B.; Fau, S.; Perera, A.; Bartlett, R. J. Gas-Phase Synthesis of Boronylallene ($H_2CCCH(BO)$) under Single Collision Conditions: A Crossed Molecular Beams and Computational Study. *J. Phys. Chem. A* **2014**, DOI: 10.1021/jp501595.

(12) Balucani, N.; Asvany, O.; Kaiser, R. I.; Osamura, Y. Crossed Beam Reaction of Cyano Radicals with Hydrocarbon Molecules V: Formation of Three C_4H_3N Isomers from Reaction of CN(X^2S^+) with Allene, H_2CCCH_2 (X^1A_1), and Methylacetylene, CH_3CCH (X^1A_1). *J. Phys. Chem. A* **2002**, *106*, 4301−4311.

(13) Dobrijevic, M.; Hebrard, E.; Loison, J. C.; Hickson, K. M. Coupling of Oxygen, Nitrogen, and Hydrocarbon Species in the Photochemistry of Titan's Atmosphere. *Icarus* **2014**, *228*, 324−346.

(14) Bhetanabhotla, M. N.; Crowell, B. A.; Coucouvinos, A.; Hill, R. D.; Rinker, R. G. Simulation of Trace Species Production by Lightning and Corona Discharge in Moist Air. *Atmos. Environ.* **1985**, *19*, 1391−1397.

(15) Yang, D. L.; Koszykowski, M. L.; Durant, J. L., Jr. The Reaction of NH_2 (X^2B_1) with O(^{3}P): A Theoretical Study Employing Gaussian 2 Theory. *J. Chem. Phys.* **1994**, *101*, 1361−1368.

(16) Duan, X.; Page, M. *Ab Initio* Variational Transition State Theory Calculations for the O+NH_2 Hydrogen Abstraction Reaction on the $^4A'$ and $^4A''$ Potential Energy Surfaces. *J. Chem. Phys.* **1995**, *102*, 6121−6127.

(17) Sumathi, R.; Sengupta, D.; Nguyen, M. T. Theoretical Study of the H_2 + NO and Related Reactions of [H_2NO] Isomers. *J. Phys. Chem. A* **1998**, *102*, 3175−3183.

(18) Kurosaki, Y.; Takayanagi, T. Ab Initio Molecular Orbital Study of the N(^{2}D) + H_2O Reaction. *J. Phys. Chem. A* **1999**, *103*, 436−442.

(19) Kurosaki, Y.; Takayanagi, T. *Ab Initio* Molecular Orbital Study of Potential Energy Surface for the $H_2NO(^2B_1)$ →NO($^2\Pi$)+H_2 Reaction. *J. Mol. Struct.: THEOCHEM* **2000**, *507*, 119−126.

(20) Homayoon, Z.; Bowman, J. M. A Global Potential Energy Surface Describing the N(^{2}D) + H_2O Reaction and a Quasiclassical Trajectory Study of the Reaction to NH + OH. *J. Phys. Chem. A* **2014**, *118*, 545−553.

(21) Umemoto, H.; Asai, T.; Hashimoto, H.; Nakae, T. Reactions of N(^{2}D) with H_2O and D_2O; Identification of the Two Exit Channels, NH(ND) + OH(OD) and H(D) + HNO(DNO). *J. Phys. Chem. A* **1999**, *103*, 700−704.

(22) Casavecchia, P.; Balucani, N.; Cartechini, L.; Capozza, G.; Bergeat, A.; Volpi, G. G. Crossed Beam Studies of Elementary Reactions of N and C Atoms and CN Radicals of Importance in Combustion. *Faraday Discuss.* **2001**, *119*, 27−49.

(23) Braams, B. J.; Bowman, J. M. Permutationally Invariant Potential Energy Surfaces in High Dimensionality. *Int. Rev. Phys. Chem.* **2009**, *28*, 577−606.

(24) Yang, J.; Shao, K.; Zhang, D.; Shuai, Q.; Fu, B.; Zhang, D. H.; Yang, X. Trapped Abstraction in the O(^{1}D) + CHD_3 → OH + CD_3 Reaction. *J. Phys. Chem. Lett.* **2014**, *5*, 3106−3111.

(25) Lambert, R. M. Mass-Spectrometric Study of the System H + NO. *Chem. Commun.* **1966**, *23*, 850−851.

(26) Kutina, R. E.; Goodman, G. L.; Berkowitz, J. Photoionization Mass Spectrometry of NH_2OH: Heats of Formation of HNO^+ and NOH^+. *J. Chem. Phys.* **1982**, *77*, 1664−1676.

(27) McLean, A. D.; Loew, G. H.; Berkowitz, D. S. HNO^+ and NOH^+ Potential Energy Surfaces for the Lowest Two Electronic States Including the Barrier to Isomerization. *Mol. Phys.* **1978**, *36*, 1359−1372.

(28) Aoiz, F. J.; Banares, L.; Castillo, J. F.; Herrero, V. J.; Martinez-Haya, B.; Honvault, P.; Launay, J. M.; Liu, X. H.; Lin, J. J.; Harich, S.; Wang, C. C.; Yang, X. The O(^{1}D)+H_2 Reaction at 56 meV Collision Energy: A Comparison between Quantum Mechanical, Quasiclassical Trajectory, and Crossed Beam Results. *J. Chem. Phys.* **2002**, *116*, 10692−10703.